ISSN 0016-7932, Geomagnetism and Aeronomy, 2016, Vol. 56, No. 4, pp. 381–392. © Pleiades Publishing, Ltd., 2016.
Original Russian Text © B.B. Gvozdevskii, A.A. Abunin, P.G. Kobelev, R.T. Gushchina, A.V. Belov, E.A. Eroshenko, V.G. Yanke, 2016, published in Geomagnetizm i Aeronomiya, 2016, Vol. 56, No. 4, pp. 411–422.

Magnetospheric Effects of Cosmic Rays. 1. Long-Term Changes in the Geomagnetic Cutoff Rigidities for the Stations of the Global Network of Neutron Monitors

B. B. Gvozdevskii[a], A. A. Abunin[b], P. G. Kobelev[b], R. T. Gushchina[b], A. V. Belov[b], E. A. Eroshenko[b], and V. G. Yanke[b]

[a] *Polar Geophysical Institute, Russian Academy of Sciences, Apatity, Russia*

[b] *Institute of Terrestrial Magnetism, Ionosphere and Radio Wave Propagation, Russian Academy of Sciences, Troitsk, Russia*

e-mail: yanke@izmiran.ru; gvozdevsky@pgia.ru; abunin@izmiran.ru; kosmos061986@yandex.ru; rgus@izmiran.ru; abelov@izmiran.ru; erosh@izmiran.ru

Received August 13, 2015; in final form, January 6, 2016

Abstract—Vertical geomagnetic cutoff rigidities are obtained for the stations of the global network of neutron monitors via trajectory calculations for each year of the period from 1950 to 2020. Geomagnetic cutoff rigidities are found from the model of the Earth's main field *International Geomagnetic Reference Field* (IGRF) for 1950–2015, and the forecast until 2020 is provided. In addition, the geomagnetic cutoff rigidities for the same period are obtained by Tsyganenko model T89 (Tsyganenko, 1989) with the average annual values of the *Kp*-index. In each case, the penumbra is taken into account in the approximation of the flat and power spectra of variations of cosmic rays. The calculation results show an overall decrease in geomagnetic cutoff rigidities, which is associated with the overall decrease and restructuring of the geomagnetic field during the reporting period, at almost all points.

DOI: 10.1134/S0016793216040046

1. INTRODUCTION

The magnetospheric effect of cosmic rays, i.e., the response of the cosmic ray flux variations to the changes in the state of the magnetosphere, was discovered during latitude measurements conducted by J. Clay in 1927 and has by now been quite well studied. Modern development of the experiment requires more rigorous studies of magnetospheric effects in terms of both the duration of observations and the accuracy of the experimental data. This is associated, for example, with the fact that the geomagnetic field has decreased by about 4% for the sixty-year period of cosmic ray observations, and it decreases at a different rate in different regions. Overall, the magnetic field has changed dramatically since 1900. In (Xu et al., 2000), it was noted that, while the dipole moment has decreased by 6.5% since 1900, the contribution of the quadrupole and octopole has increased by 95 and 74%, respectively. In general, the contribution of higher harmonics of the field during the same period has increased by ~30%. The dipole center shifted by 200 km in the direction of the Pacific Ocean. In addition, certain features were observed in the behavior of the expansion coefficients of the higher order magnetic field. Thus, a jump in the expansion coefficients of higher order (>7) in 1945–1955 was discovered but was not observed either before or after this period.

In order to estimate the impact of such a large magnetic field adjustment in terms of magnetospheric effects of cosmic rays, it is necessary to obtain the planetary distribution of the geomagnetic cutoff rigidities for the entire observation period, with an accounting of at least the internal current systems. According to preliminary estimates, changes in the basic energy characteristic of the incoming particles, the geomagnetic cutoff rigidity, reaches ~2 GV (>10% for the equatorial detectors) in some regions, which is very important in the study of long-term variations of cosmic rays.

Two key concepts, such as the geomagnetic cutoff rigidity (for the description of isotropic variations) and the asymptotic particle reception cone (for the description of anisotropic variations), make it possible to describe all of the magnetospheric effects of cosmic rays. In the description of the long-term variations, it is sufficient to consider only the isotropic approximation. An accurate determination of the geomagnetic cutoff rigidity is crucial for the determination of spectra of primary cosmic ray fluxes.

Studies of magnetospheric effects were rapidly developing in the 1950s within the Störmer theory (Alfven and Felthammar, 1967). The discrepancy between the theoretical and experimental data (the equator of cosmic rays, latitudinal variation, and east-

west anisotropy of cosmic rays) showed that the dipole approximation of the geomagnetic field is too rough. In order to increase the accuracy of the results, the higher harmonics of the geomagnetic field should be taken into account in the calculation of the cutoff rigidities of cosmic rays. The generally accepted definition for cutoff rigidity is currently the numerical integration of motion equations of charged particles. Cutoff rigidities can be calculated by this method with an arbitrarily high degree of accuracy. Both internal and external sources of the geomagnetic field can be taken into account in the geomagnetic field approximation, which is of paramount importance in the analysis of solar cosmic rays.

An overview of magnetospheric effects at an early stage was given in (Hofmann et al., 1968; Dorman et al., 1971; Smart et al., 2000; Kudela and Bobik, 2004; Bobik et al., 2006). A review of recent works can be found in (Dorman, 2009).

An extensive and most comprehensive and systematic investigation of magnetospheric effects of cosmic rays, including long-term changes, was carried out by Shea Smart (1967–2007). Global distributions of the vertical geomagnetic cutoff rigidity in steps of $5^\circ \times 15^\circ$ by latitude and longitude for the epochs of 1955, 1965, 1975, 1980 (Shea and Smart, 1967, 1975a, b, 1983) and 1990, 1995, 2000 (Smart and Shea, 1997, 2007a, b) were computed for the respective epochs and trajectory calculations based on the geomagnetic field model. Vertical geomagnetic cutoff rigidities were obtained for all stations of the global network for nine five-year epochs in 1955–1995 (Shea and Smart, 2001).

Shea and Smart (1975b) noticed the uneven distribution of changes in the planetary distribution of geomagnetic cutoff rigidities for 20 years from 1955 to 1975, especially in the northern and southern parts of the Atlantic Ocean. In the southern part of the Atlantic Ocean, a decrease in rigidity was observed, while a comparable increase in the vertical cutoff rigidity occurred in the northern part.

Such calculations were not conducted for the existing network of detectors over the past four epochs. In addition, over the past 20 years, about a third of the new neutron monitors were added to the system and a network of multidirectional muon telescopes was created; the geomagnetic cutoff rigidity and asymptotic reception cones for these should be determined for the first time for all detectors.

2. METHOD OF CALCULATION OF GEOMAGNETIC CUTOFF RIGIDITY

The geomagnetic cutoff rigidity calculations were based on the solution of equations of motion of charged particles in the geomagnetic field. As is known, there is no analytic solution of the equations of motion of charged particles even in the magnetic dipole field (except for trajectories lying in the equatorial plane). The first calculations of the trajectories of cosmic rays in the dipole approximation were carried out on an analog computer (Lemaitre and Vallarta, 1936a, b), and the transition region of the penumbra of cosmic rays was found. By developing the Störmer theory and the forbidden cone concept, they introduced the concept of the allowed cone, when all the trajectories are allowed, and the concept of the main cone, which includes the allowed cone and penumbra region. This transition region is a complex alternation of irregular forbidden and allowed directions of arrival of particles. The calculations of the trajectories of cosmic rays in an approximation to the real geomagnetic field represented by six spherical functions were carried out in (Jory, 1956). Currently, the generally accepted and the most accurate way to determine the geomagnetic cutoff rigidity is the method of trajectory calculations based on the solution of the equation of motion of charged particles in the geomagnetic field.

The problem of motion of charged particles in the magnetosphere of the Earth was solved as described in (Shea et al., 1965). The equation of motion was solved numerically by the Runge–Kutta method on the fourth order of accuracy with adaptive step (Forsythe et al., 1980). The initial data were the geographical coordinates of the station and the components of the initial vector of the particle velocity. The particles start from a height of 20 km. Integration is completed in three cases: either a particle penetrates to a depth of less than $(R_E + 20)$ km (R_E is the radius of the Earth) (the particle returns back into the atmosphere, trajectory *0*, Fig. 1), the integration is completed at the end of the target time (the particle is considered captured, trajectory *1*), or the particle crosses the surface of the magnetopause (moves beyond the magnetosphere, trajectories *2–5*). In the latter case, the trajectory is defined as allowed, otherwise, as forbidden. As a result of the calculation, a discrete penumbra function $g(R)$ is formed; it takes values "0" or "1" for all rigidity values with the selected step of 0.001 GV. When selecting the integration step, we proceeded from the fact that the calculation error at each step should be an order of magnitude lower than the expected result, and according to our estimates and data from other works the expected result is 0.01 GV.

Geomagnetic cutoff rigidities were calculated with an annual resolution from 1950 through 2020. For this purpose, a model of the main magnetic field IGRF was used. This model is developed until 2015 for every five years. It takes into account secular variations of the magnetic field. The model continues until 2020 (IGRF-12 model, 2015). The field is represented by ten or 13 spherical harmonics, but we limited ourselves to ten harmonics for the entire period and to eight harmonics for the predictive model of the field. In addition, in order to estimate the effect of long-term changes in the external magnetic fields, geomagnetic cutoff rigidities for Tsyganenko model T89 (Tsyganenko, 1989) in which

the *Kp*-index determined by the average annual values of *Ap*-index was used as a parameter were calculated,.

An important consideration when calculating the geomagnetic cutoff rigidities is the account of the penumbra region, which is made by the introduction of the effective cutoff rigidity.

The effective geomagnetic cutoff rigidity can be defined in different ways. In the simplest case, it is possible to carry out a simple summation of the allowed and forbidden regions defined by the penumbra region. This summation can be carried out more correctly with use of the expected spectrum of cosmic rays as a weighting function. This is true outside the atmosphere. In order to account for meteorological factors, the effect of the atmosphere should be additionally included in the weighting function, which is convenient to do with coupling functions.

In the general case, with the spectrum of variations $\delta J/J$ and the influence of the atmosphere (which is taken into account by the method of coupling functions $W(R, h)$), the effective rigidity of the geomagnetic cutoff R_{eff} is determined by the following equation

$$\int_{R_{\text{eff}}}^{R_H} W(R,h)\delta J/J(R)dR = \int_{R_S}^{R_H} g(R)W(R,h)\delta J/J(R)dR, \quad (1)$$

where R_H and R_S are magnetic rigidities of the main and Störmer cones and $g(R)$ is the penumbra function, which is equal to "0" or "1" for the forbidden or allowed regidities, respectively.

In order to solve the equation with respect to R_{eff}, the spectrum of variations is approximated by a power function $\delta J/J = aR^{-\gamma}$, and the atmospheric influence is taken into account through the coupling function, which in a relatively small region of the penumbra is well approximated by the power function $W(R) = cR^{\eta}$ (Fig. 2). Then, by integrating we obtain

$$R_{\text{eff}}^{\gamma+\eta+1} = R_H^{\gamma+\eta+1} - (\gamma+\eta+1)\int_{R_S}^{R_H} g(R)R^{\eta+\gamma}dR. \quad (2)$$

In the particular case of the primary spectrum independent of the energy of cosmic rays (white or flat spectrum, i.e., $\gamma = 0$) and by neglecting the atmospheric influence (i.e., $\eta = 0$), we obtain an expression for the effective geomagnetic cutoff rigidity

$$R_{\text{eff}} = R_H - \int_{R_S}^{R_H} g(R)dR. \quad (3)$$

The case of the white spectrum of variations of cosmic rays is not physically implemented, but when there are no strict requirements on the accuracy of such calculations, effective cutoff rigidities are convenient and often used.

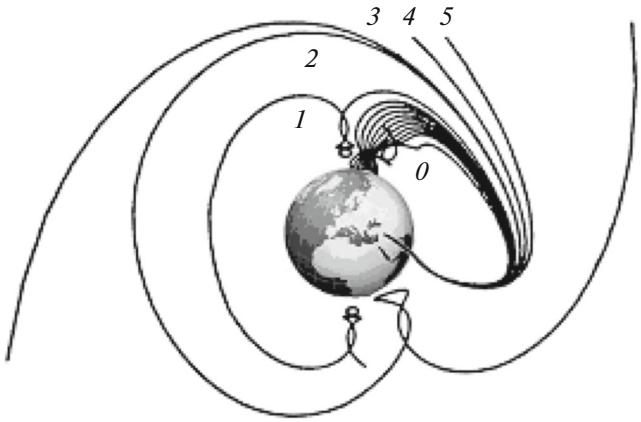

Fig. 1. Example of the possible trajectories of particles in the geomagnetic field.

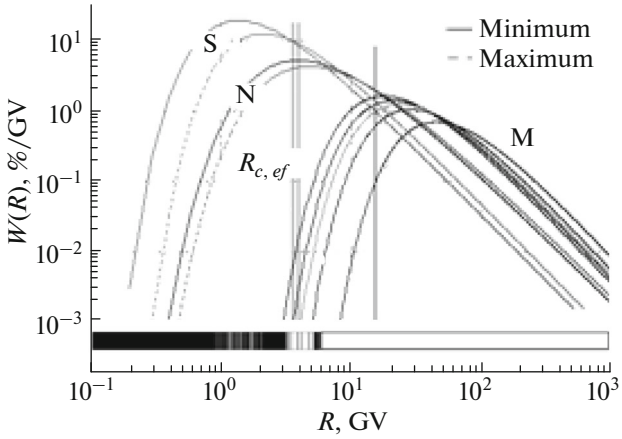

Fig. 2. Illustration of a methodology for the estimation of the effective cutoff rigidity taking into account the penumbra (at the lower part of the figure) of cosmic rays. Coupling function for three types of detectors are given: N is the neutron monitor, M is the muon telescope, and S are the stratospheric measurement.

It follows from the above that the penumbra width influences the result of the calculation of the effective rigidity of the geomagnetic cutoff, both with exclusion of and accounting for the range of variations and the effect of the atmosphere. This circumstance leads to the fact that it is impossible to characterize any point on the Earth by some universal geomagnetic cutoff rigidity. It is different for different instruments and changes with time.

The planetary variation of the penumbra width (right scale in the GV) as calculated by the IGRF model for the epoch 2015 is shown in Fig. 3.

Figure 3 shows that, in the real magnetic field, the structure of the penumbra region and the planetary

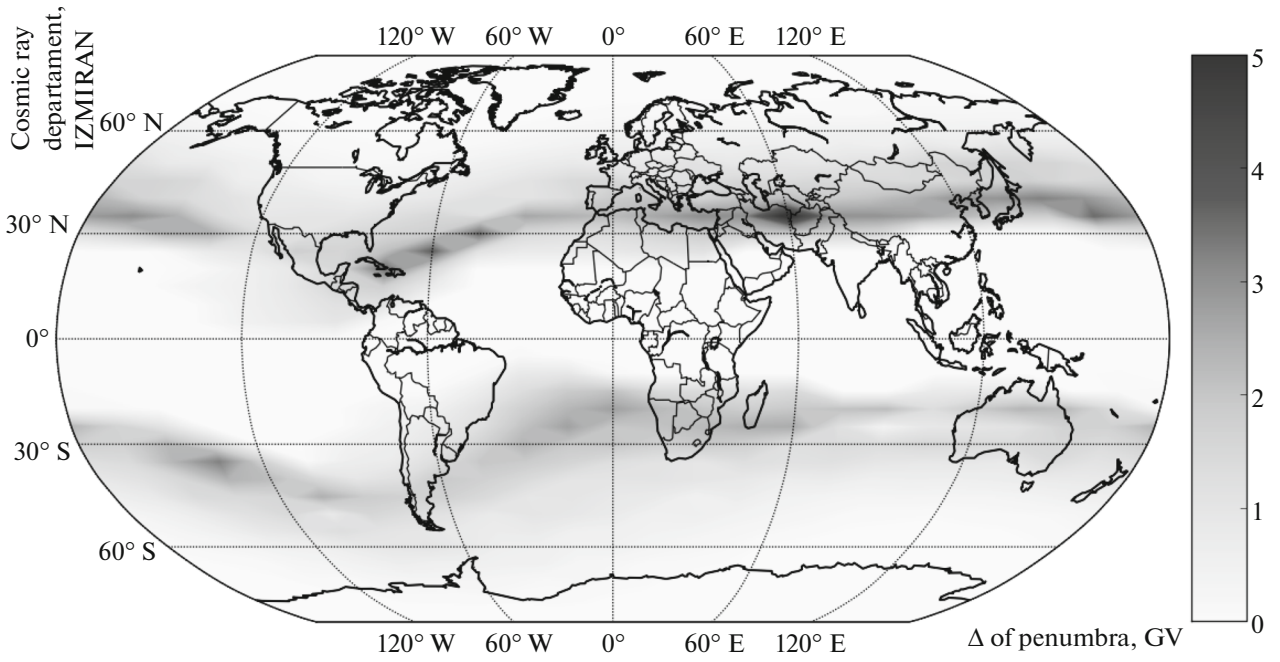

Fig. 3. Planetary variation of the penumbra region width (right scale in GV) for the 2015 epoch in the IGRF model.

change of its width are very complex. In the eastern part of the Northern Hemisphere, the width of the penumbra reaches 4 GV, while the width is much smaller in the eastern part of the Southern Hemisphere but the penumbra is observed up to the polar latitudes. Figure 4 shows the dependence of the penumbra width on the geomagnetic cutoff rigidity. It is interesting that an almost deterministic relationship is observed between the width of the penumbra and the geomagnetic cutoff rigidity. In (Shea and Smart, 1975b), this dependence was also given, but it was much less deterministic, apparently, because of the use of the integration step in the penumbra of 0.01 GV. Interestingly, the rigidity dependence of the penumbra width for the two given epochs remained almost the same, even though there have been great changes in the overall magnetic field for this time scale in over a hundred years.

3. RESULTS AND DISCUSSION

Before proceeding to the calculation of the geomagnetic cutoff rigidity for the network of stations of neutron monitors, the planetary distributions of geomagnetic cutoff rigidities were calculated for the IGRF for all epochs from 1950 to 2020 with a steps of five years for the grid 5° × 15° in latitude and longitude. Digital and graphical results can be found on the website (Magnitospheric effect 2015). Such distributions make it possible to visualize the dynamics of changes in geomagnetic cutoff rigidities. In addition, planetary distributions by the interpolation make it possible to simply obtain geomagnetic cutoff rigidities for any points, if it is possible to confine ourselves to the accuracy of a few tenths of GV. The interpolation can be carried out, for example, based on the Lagrange interpolation formula for the four points. Changes in the planetary distribution of the vertical geomagnetic cutoff rigidity for the epoch 2015 relative to the epoch 1950 is shown in Fig. 5, i.e., during the entire period of continuous monitoring of cosmic rays. Figure 5 shows anomalies of changes in the geomagnetic cutoff rigidities in the northern (increase of rigidity) and southern (decrease of rigidity) Atlantic.

In analysis of Fig. 5, a significant increase in geomagnetic cutoff rigidities from the east coast of North America down to Gibraltar and a significant decrease in geomagnetic cutoff rigidities in the area of South America, as well as the formation of two big features concentrated mainly in the northern and southern waters of the Atlantic Ocean, can be noted. There are no cosmic ray detectors at the epicenter of these formations, where changes in geomagnetic cutoff rigidities reach almost 3 GV, but the changes in the cutoff rigidity are significant even at the periphery of these structures. Thus, the periphery of the region in the North Atlantic includes many American and Canadian stations and part of the European stations. In general, for all of these points, the rigidity increases to 1 GV. In the southern part of the Atlantic Ocean, the decrease of geomagnetic cutoff rigidities is even greater and reaches 2 GV.

The isolines of the vertical geomagnetic cutoff rigidity for the epoch 2015 are shown in Fig. 6.

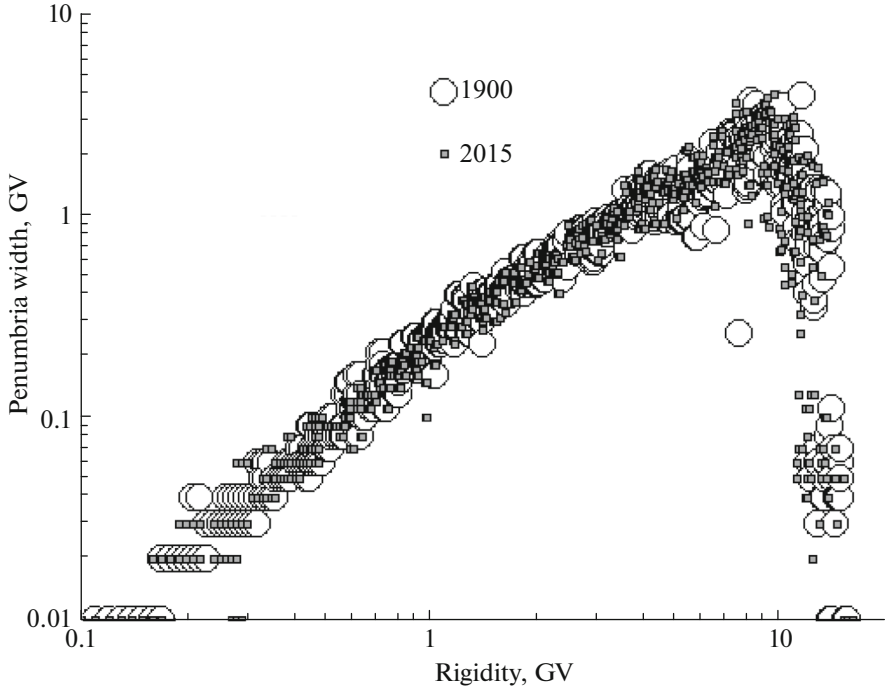

Fig. 4. Dependence of the penumbra width on the cutoff rigidity. Large open circles refer to the epoch 1900, squares, to the epoch 2015.

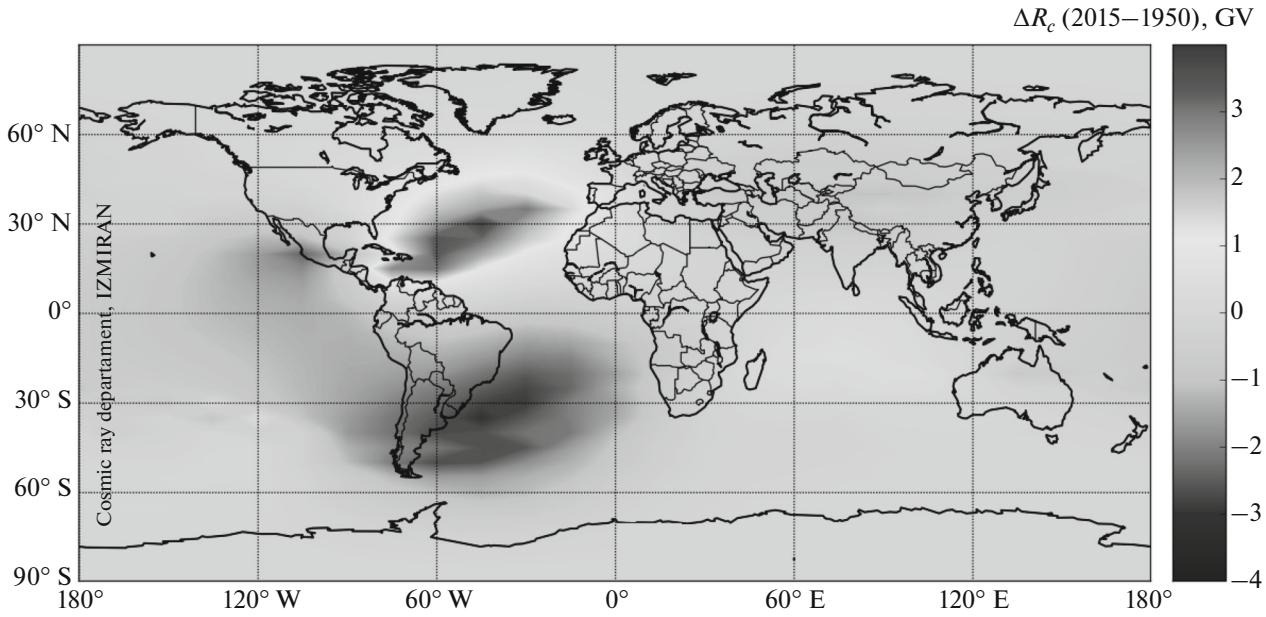

Fig. 5. Changes in the planetary distribution of the vertical geomagnetic cutoff rigidity for the epoch 2015 with respect to the epoch 1950.

Changes in the geomagnetic cutoff rigidities of the global network of cosmic ray stations are given in Fig. 7, the results of which were obtained for the IGRF. The figure shows the changes in geomagnetic cutoff rigidities with respect to the epoch 1950 for the entire period of continuous monitoring of cosmic rays for four groups of stations of cosmic rays. The temporal changes of geomagnetic cutoff rigidities of high-latitude detectors (<3 GV) reach 0.5 GV, with different signs. For the American, Canadian, and European

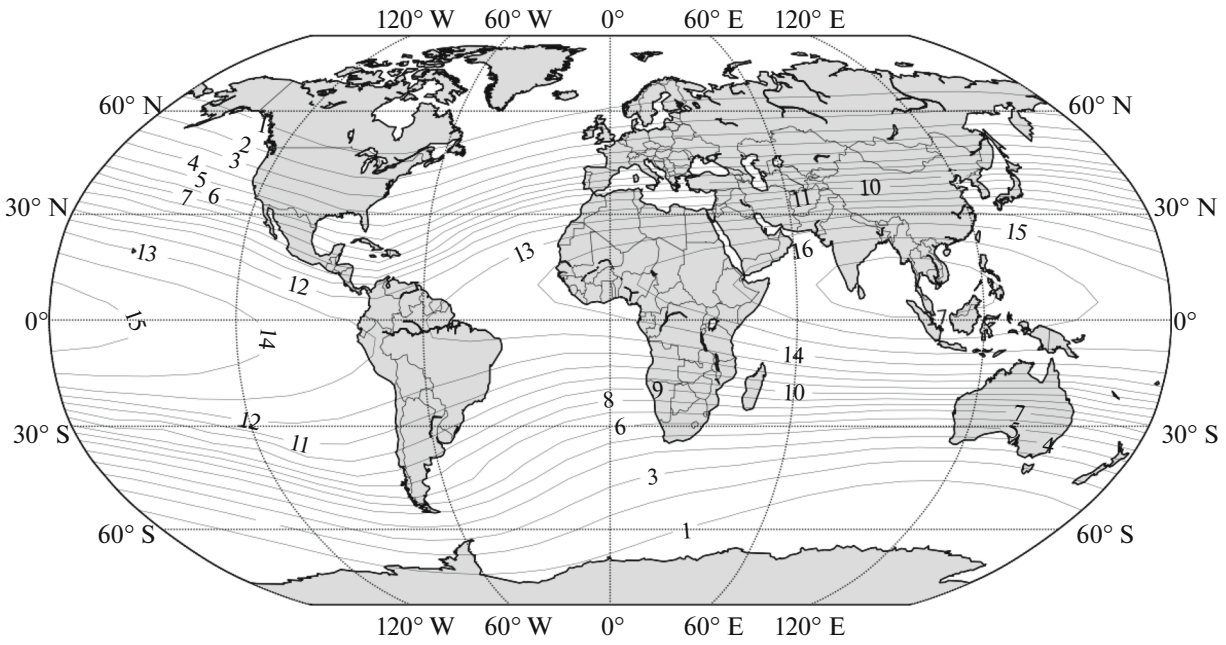

Fig. 6. Isolines of the vertical geomagnetic cutoff rigidity for the epoch 2015.

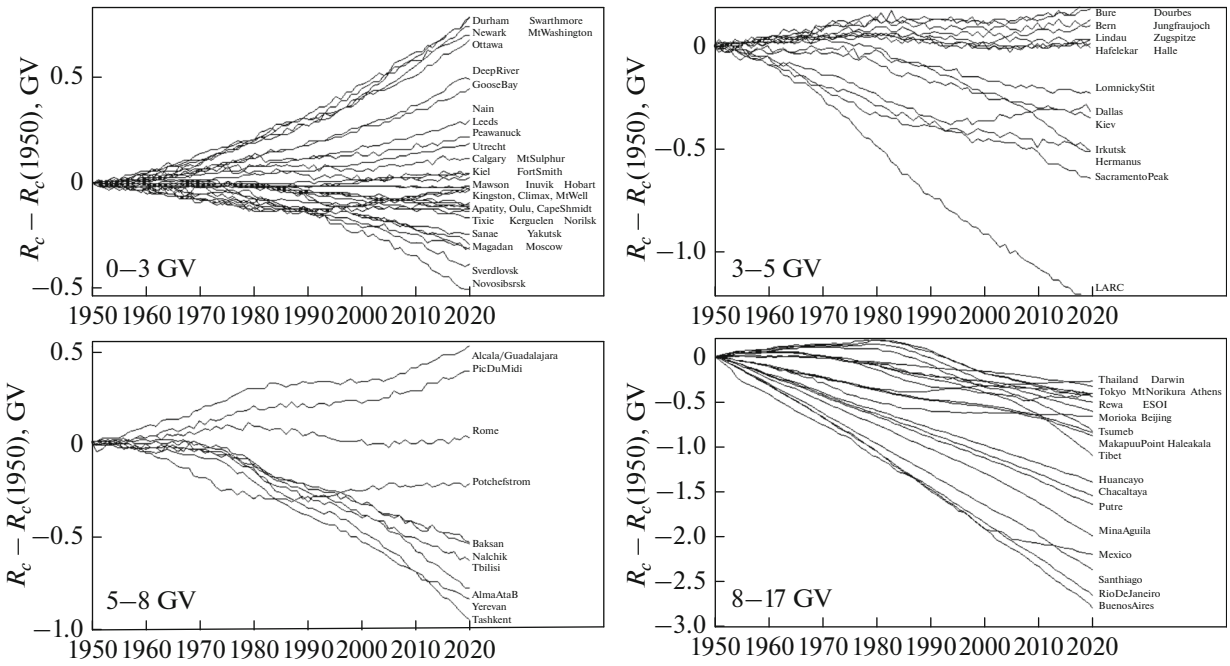

Fig. 7. Changes in vertical geomagnetic cutoff rigidities for four groups of stations of cosmic rays with respect to the epoch 1950 (in the approximation of the IGRF and the flat spectrum of variations).

stations, a systematic increase of cutoff rigidities is observed. This is because of the influence of the peripheral abnormal region in the northern part of the Atlantic, as seen in Fig. 5. For other detectors, there is a slight decrease of cutoff rigidities. For intermediate values in the range of 3–8 GV, geomagnetic cutoff rigidities generally decrease, with the exception of several detectors of the western coast of Europe, an area that is the periphery of the North Atlantic anomaly. In low-latitude regions up to the equatorial, a significant decrease in geomagnetic cutoff rigidities is also observed for all detectors. Thus, there is a global decrease in geomagnetic cutoff rigidities with the exception of the North Atlantic anomaly.

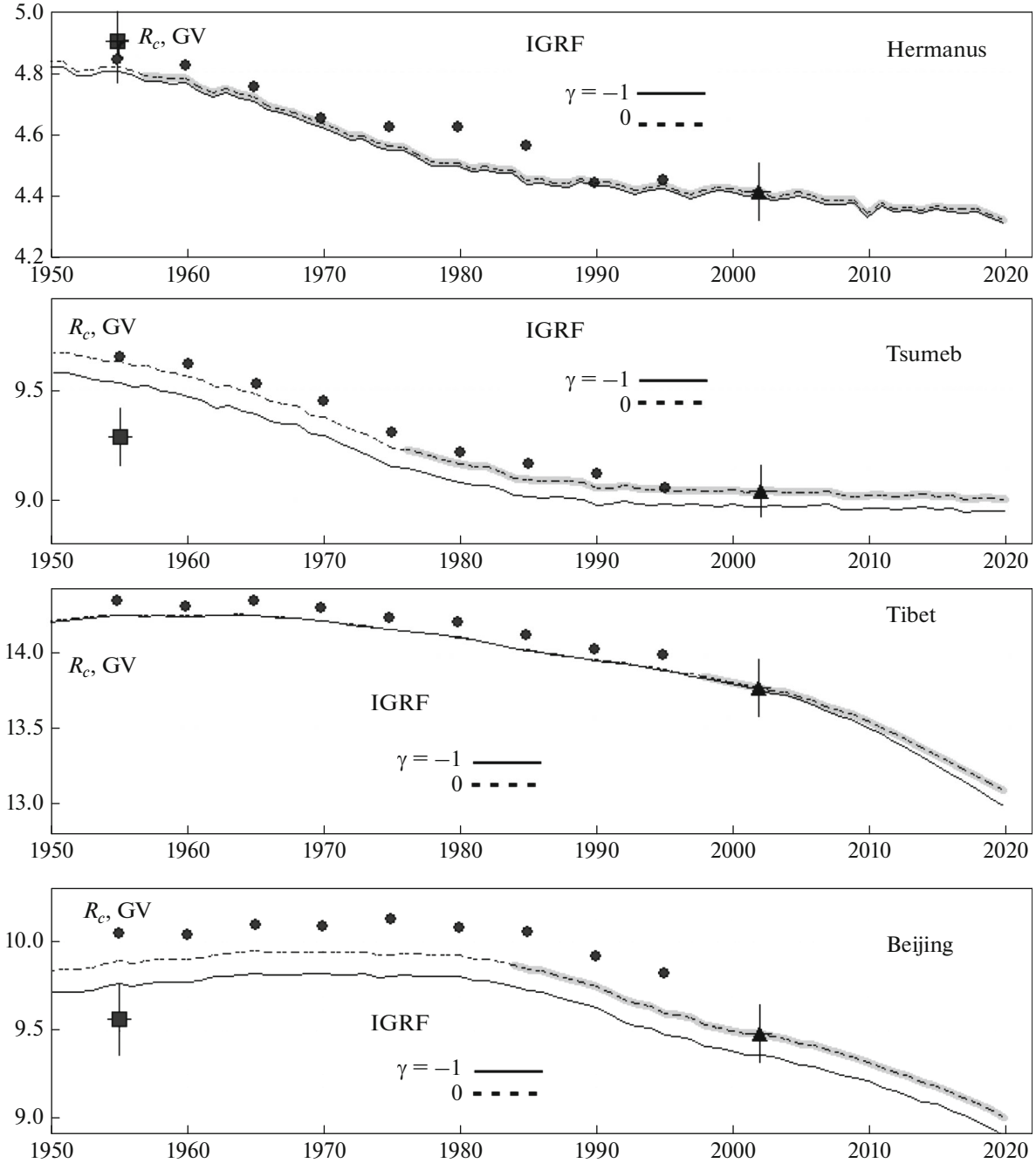

Fig. 8. Changes in the cutoff rigidity for Hermanus and Tsumeb stations and Tibet and Beijing stations. The IGRF magnetosphere model takes into account the penumbra in the approximation of the flat ($\gamma = 0$) and power ($\gamma = -1$) spectra of variations of cosmic rays.

More detailed vertical geomagnetic cutoff rigidities for each year of operating or long-operating neutron monitors of the global network in 1950–2020 were obtained by trajectory calculations. The total number of stations is 123. Geomagnetic cutoff rigidities were obtained based on the IGRF model for the period from 1950 to 2015 and the predictive model up to 2020 The results for all detectors can be found on the server (Magnitospheric effect 2015).

In Fig. 8, as an example for some of the detectors, a more detailed time course of the cutoff rigidity is shown, and the calculation results are compared with these of other authors. In each case the pair of curves refers to calculations by the IGRF model and takes into account the penumbra in two approximations: in approximation of flat ($\gamma = 0$, dashed line) and power spectra of variations of cosmic rays ($\gamma = -1$, solid curve). This pair of curves is almost identical for the

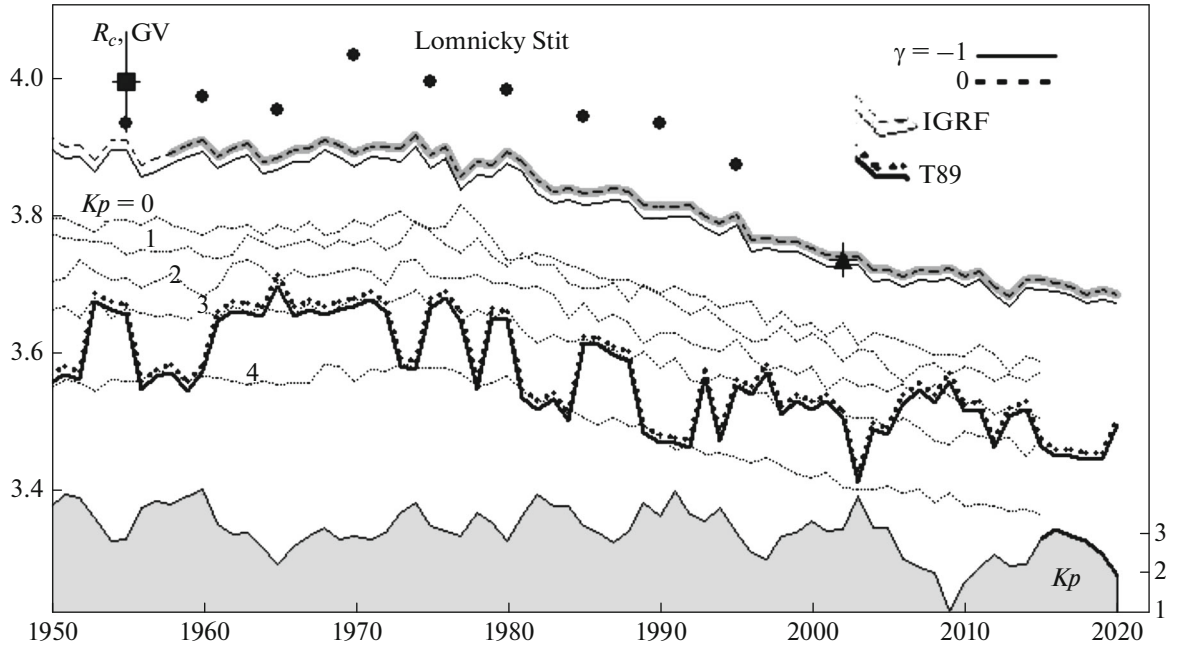

Fig. 9. Changes in the geomagnetic cutoff rigidity for the Lomnicky Stit station for two magnetosphere models (IGRF and T89) taking into account the penumbra in the approximation of the flat (γ = 0) and power (γ = –1) spectra of variations of cosmic rays.

Hermanus but differs greatly for Tsumeb. This is because of the large width of the penumbra for the Tsumeb station (Fig. 8), which leads to a greater sensitivity to variation spectrum. The estimation of accuracy gives a value of ~0.1 GV (the graph shows the error only for a single point, the 2002 epoch). For each of the detectors, the station operating period is grayed out on one of the upper curves. The results are compared with the data of the first trajectory calculations (Shea et al., 1965) obtained for the expansion of the magnetic field on the first six harmonics of the 1955 epoch (square). The circles show the results obtained from trajectory calculations (Shea and Smart, 2001) for all stations of the global network. The integration step of motion equations is 0.01 GV, and the penumbra is taken into account in the approximation of the flat spectrum of variations of cosmic rays. Our calculations give ~0.1 GV less rigidity, which we associate with a more accurate integration of the equations of motion in the penumbra region (integration step of 0.001 GV). As an example, another pair of detectors from Tibet and Beijing stations, which also vary in the penumbra width, can be cited.

The accuracy of the calculation of geomagnetic cutoff rigidities depends on three factors: the accuracy of the geomagnetic field representation, the error of the integration method of equations of motion of particles in this field, and the accuracy of the account for the penumbra region. The main contribution to the error is made by the error of accounting for penumbra, then the quite well-controlled error of the integration of equations of motion of particles, and finally the accuracy of the geomagnetic field representation. The overall calculation error in the rigidity range of 5–12 GV is 0.15 GV and a little smaller outside this interval.

At this stage, we took into account only the internal magnetic field and its variation. However, the external field is also subject to long-term changes that should be estimated.

5. CONTRIBUTION OF THE EXTERNAL MAGNETIC FIELD IN LONG-TERM CHANGES OF THE THRESHOLD RIGIDITY

The Earth's magnetosphere is subject to long-term changes caused by solar activity. In order to estimate these changes, the Tsyganenko model of the magnetic field can be used, for example, T89 (Tsyganenko, 1989). The input parameter of this model is the *Kp*-index. Since the *Kp*-index is the logarithmic index, annual average values of the *Ap*-index were used in order to obtain annual averages of the *Kp*-index with the corresponding recalculation.

In Fig. 9, the results of calculations for mid-latitude station Lomnicky Stit are compared by models IGRF and T89. The notation is the same as in Fig. 8. The top of Fig. 9 also shows the result of calculations by the IGRF model and a comparison with the results of other authors (marked with circles).

The middle part of Fig. 9 shows geomagnetic cutoff rigidities by the Tsyganenko model T89 (Tsyganenko, 1989). The values of the *Kp*-index (from 0 to 4 points) show the possible corridor of changes of geomagnetic cutoff rigidities, within which the actual values change

depending on the value of the *Kp*-index. The lower part of Fig. 9 shows the average value of the *Kp*-index. For the period from 2015 to 2020 marked by the bold line in the lower part of Fig. 9, we used predicted values of the *Kp*-index.

The calculation shows that an accounting for the influence of the outer magnetosphere on long-term changes of cutoff rigidities reduces geomagnetic cutoff rigidities by a few tenths of GV and reaches about 0.3 GV for high-latitude detectors, for example, Kerguelen, Deep River, Durham, and Apatity stations. All observed changes in the cutoff rigidity are in opposition to the changes of the *Kp*-index. For mid-latitude stations, this influence is reducesd(Fig. 10) and vanishes for low-latitude detectors.

6. COMPARISON WITH THE RESULTS OF OTHER AUTHORS AND ESTIMATION OF THE ACCURACY OF CALCULATIONS

In the study of solar cosmic rays, it was necessary to carry out individual trajectory calculations for each event. These calculations were carried out by many researchers. In the case of galactic cosmic rays, it is sufficient to carry out trajectory calculations for the annual averaging for the global network of detectors.

In Figs. 8–10, the results of different authors were compared for the individual stations. On the global scale, it was carried out in Fig. 11 for the 1980 epoch in a comparison of the calculations of this paper with the calculations in (Shea and Smart, 1983). A slight difference in a few tenths of GV is observed only in the penumbra. This is probably because of the different integration step of equations of motion of particles in the penumbra region (0.001 GV in this paper and 0.01 GV in (Shea and Smart, 1983)).

During the trajectory calculations of geomagnetic cutoff rigidities for the period of 2015–2020, the predicted Earth's magnetic field was used; this is also the result of the IGRF-12 model (IGRF-12 Model, 2015). A question about the accuracy of geomagnetic cutoff rigidities determined based on predictive models arises. For this purpose, the difference between geomagnetic cutoff rigidities R_c (based on the IGRF-11,12 model for 2015) and R_c (*forecast*) (based on forecast by the IGRF-11,12 model for 2015) was found. This difference does not exceed 0.1 GV, i.e., the accuracy of numerical calculations. The planetary distribution of this estimation is shown in Fig. 12.

In recent years, Internet projects of online calculators of geomagnetic cutoff rigidities have been actively developed, for example, (Zreda, 2012) and (Boschini et al., 2014), although such projects do not allow for massive calculations. The project in (Zreda, 2012) is based on the IGRF model, and the result for some detectors is shown in Fig. 10 (large hollow circles). There is a large discrepancy with the results of other authors, especially for equatorial detectors. The second project (Boschini et al., 2014) is based on more complex magnetosphere models T96 (Tsyganenko et al., 1996). This project also makes it possible to calculate geomagnetic cutoff rigidities for T02 models (Tsyganenko, 2002a, b) and T05 models (Tsyganenko and Sitnov, 2005) with automatic use of the necessary input parameters of the interplanetary medium for the magnetosphere model. Therefore, it is impossible to carry out a valid comparison for our case. An overview of the models can be found in (Tsyganenko, 2013).

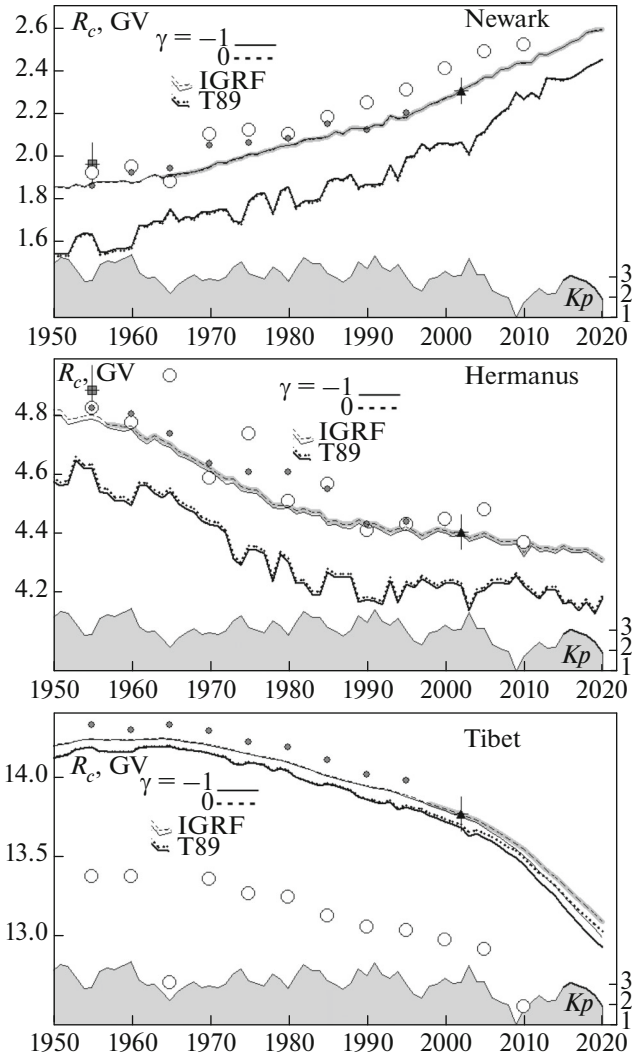

Fig. 10. Changes in the cutoff rigidity for Newark, Hermanus, and Tibet stations. Notation is the same as in Fig. 9. Transparent circles are the results of an online calculator (Zreda, 2012).

7. CONCLUSIONS

The reason for the significant change in geomagnetic cutoff rigidities in 1955–2020 is a general decrease in the magnetic field of the Earth, against the background of which a certain "contrast" increases

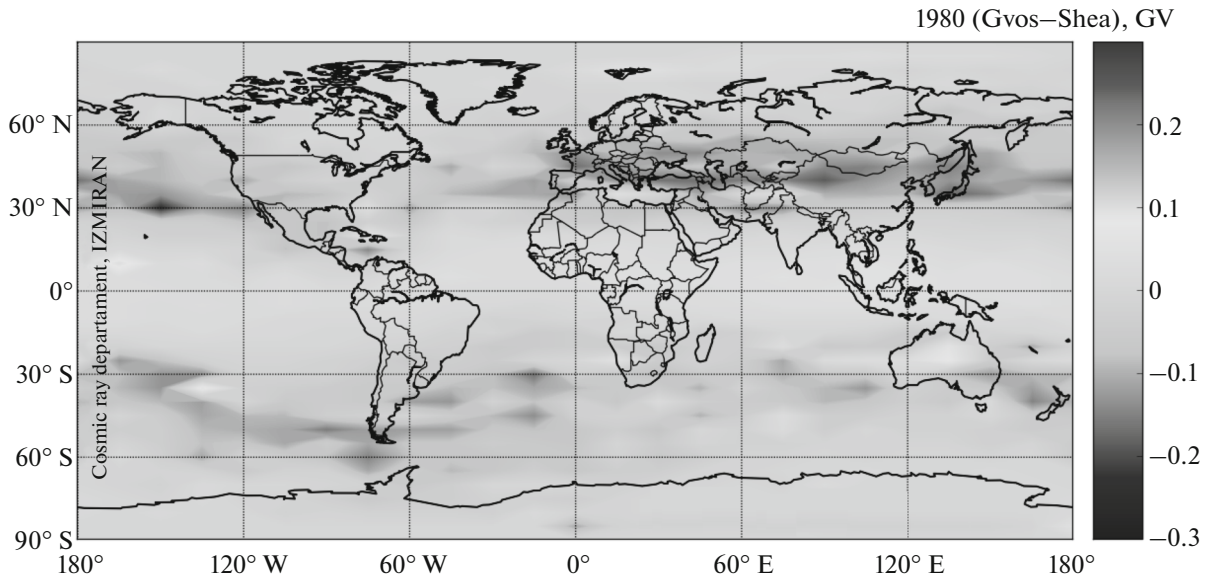

Fig. 11. Difference in geomagnetic cutoff rigidities (the right scale in the GV) calculated in this paper and in (Shea and Smart, 1983) for the 1980 epoch.

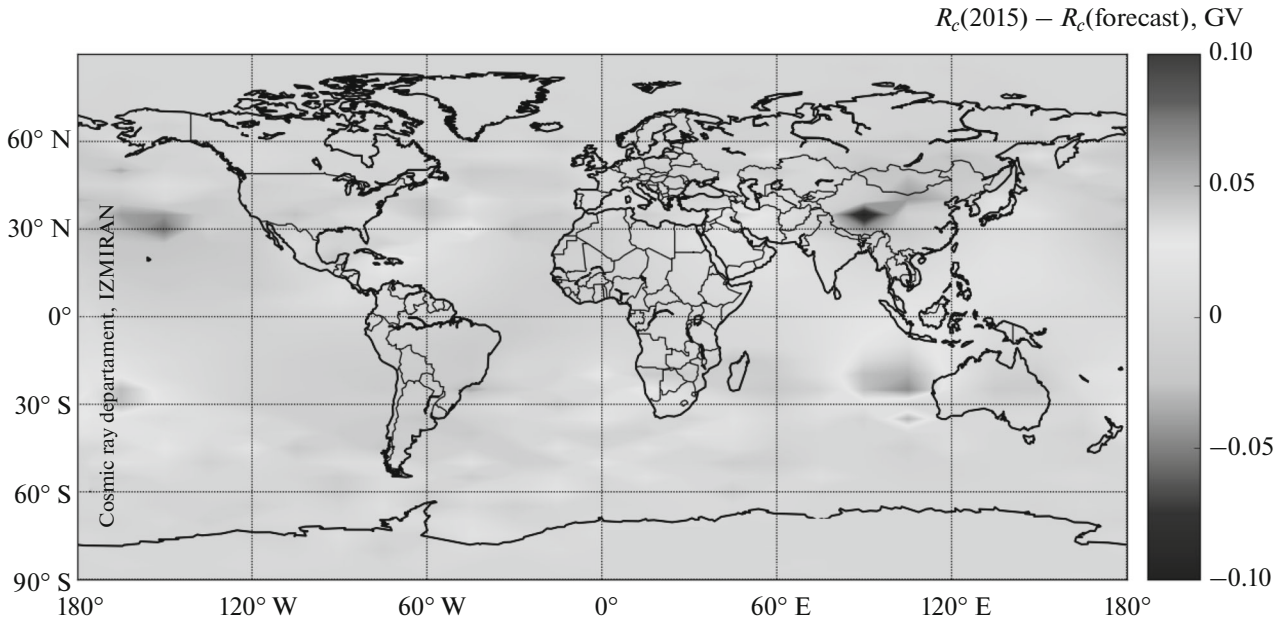

Fig. 12. Errors in the calculation of geomagnetic cutoff rigidities according to the prognostic magnetic field of the IGRF-12 model for the 2015 epoch.

with the presence of regions with a sharp change in the field near the poles and magnetic anomalies, as well as changes in the displacement vector of the poles and anomalies.

The long-term changes in effective geomagnetic cutoff rigidities for the global network of neutron monitors are significant and generally lead to a decrease. It should be taken into account when estimating the spectrum of long-period variations.

The effect of the outer magnetosphere on long-term changes in cutoff rigidities leads to a slight decrease in the geomagnetic cutoff rigidity. The observed 11-year cut-off rigidity changes are in opposite phase with the change of the *Kp*-index, are insignificant, and do not exceed 0.1 GV.

All of the obtained results are published in the graphic and digital forms on the website (Magnitospheric effect, 2015).

First of all, these are computations of the planetary distribution of geomagnetic cutoff rigidities for the IGRF model with the grid of 5° in latitude and 15° in longitude for periods from 1955 to 2015 in steps of 5 years and the forecast for 2020. The penumbra region was taken into account for the flat spectrum of variations of cosmic rays. In order to study the dynamic changes of the planetary distribution of geomagnetic cutoff rigidities, *AnimationGRID.gif* was created and can be found on the same website.

In addition, the geomagnetic cutoff rigidities for 123 detectors of the global network of neutron monitors are published on the website (Magnitospheric effect, 2015) for the entire observation period in steps of one year. Results were obtained for the detectors operating at the moment or long-operating detectors in the previous period. Geomagnetic cutoff rigidities were obtained for IGRF and T89 models. The penumbra region was accounted for the flat and power spectra taking into account the atmospheric influence. For ease of viewing of the changes in geomagnetic cutoff rigidities, *AnimationSTATION.gif* was also created and published on the website (Magnitospheric effect 2015).

In this paper, we restricted ourselves to long-term changes in geomagnetic cutoff rigidities, which is sufficient for the description of isotropic variations. The problem of long-term changes of asymptotic particle reception cones for the description of anisotropic variations of cosmic rays should be further investigated.

ACKNOWLEDGMENTS

This study was supported in part by the Basic Research Program of the Presidium of the Russia Academy of Sciences, project no. 23 "High-Energy Physics and Neutrino Astrophysics" and was carried out on the unique installation CRS Network, http://www.ckp-rf.ru/usu/433536/(no. 85).

REFERENCES

Alfvén, H. and Felthammar, C.-G, *Cosmic Electrodynamics. Fundamental Principles*, Oxford: Clarendon, 1963; Moscow: Mir, 1967.

Bobik, P., Boella, G., Boschini, M.J., Gervasi, M., Grandi, D., Kudela, K., Pensotti, S., and Rancoita, P.G., Magnetospheric transmission function approach to disentangle primary from secondary cosmic ray fluxes in the penumbra region, *J. Geophys. Res.*, 2006, vol. 111, no. A5, A05205. doi 10.1029/2005JA011235

Boschini, M.J., Della, T.S., Gervasi, M., Grandi, D., Rancoita, P.G., Bobik, P., and Kudela, K., Cutoff rigidity online calculator, model T96 and T05, 2014. http://www.geomagsphere.org/geomag.

Dorman, L., Cosmic rays in magnetospheres of the Earth and other planets, *Astrophys. Space Sci. Libr.*, 2009, vol. 358. doi 10.1007/978-1-4020-9239-8

Dorman, L.I., Smirnov, V.S., and Tyasto, M.I., *Kosmicheskie luchi v magnitnom pole Zemli (Cosmic Rays in the Earth's Magnetic Field)*, Moscow: Nauka, 1971.

Forsythe, G.E., Malcolm, M.A., and Moler, C.B., *Computer Methods for Mathematical Computations*, Englewood Cliffs, New Jersey: Prentice Hall, 1977; Moscow, Mir, 1980.

Hofmann, D.J. and Sauer, H.H., Magnetospheric cosmic ray cutoffs and their variations, *Space Sci. Rev.*, 1968, vol. 8, pp. 750–803. doi 10.1007/BF00175117

Jory, F.S., Selected cosmic-ray orbits in the Earth's magnetic field, *Phys. Rev.*, 1956, vol. 103, no. 4, pp. 1068–1075.

Kudela, K. and Bobik, P., Long-term variations of geomagnetic rigidity cutoffs, *Sol. Phys.*, 2004, vol. 224, nos. 1–2, pp. 423–431. doi 10.1029/*2004JA010387*

Lemaitre, G.E. and Vallarta, M.S., On the geomagnetic analysis of cosmic radiation, *Phys. Rev.*, 1936a, vol. 49, pp. 719–726. doi 10.1029/JZ070i017p04117

Lemaitre, G.E. and Vallarta, M.S., On the allowed cone of cosmic radiation, *Phys. Rev.*, 1936b, vol. 50, pp. 493–504. doi 10.1090/S0025-5718-45-99068-5

Magnitospheric effect, 2015. ftp://crsb.izmiran.ru/Magnitospheric_Effect.

Model IGRF-12, 2015. http://www.ngdc.noaa.gov/IAGA/vmod/igrf.html.

Shea, M.A. and Smart, D.F., Worldwide trajectory-derived vertical cutoff rigidities and their application to experimental measurements for 1955, *J. Geophys. Res.*, 1967, vol. 72, no. 7, pp. 2021–2028. doi 10.1029/JZ072i007p02021

Shea, M.A. and Smart, D.F., Tables of vertical cutoff rigidities for a five degree by fifteen degree a word grid calculated for 1965, AFCRL-TR-75-0381, 1975a, no. 524.

Shea, M.A. and Smart, D.F., A five by fifteen degree world grid of calculated cosmic ray vertical cutoff rigidities for 1965 and 1975, in *Proceedings of the 14th ICRC*, München, 1975b, vol. 4, pp. 1298–1303.

Shea, M.A. and Smart, D.F., Vertical cutoff rigidities for cosmic ray stations since 1955, in *Proceedings of the 18th ICRC*, Bangalore, 1983, pp. 514–515.

Shea, M.A. and Smart, D.F., A word grid of calculated cosmic ray vertical cutoff rigidities for 1980, in *Proceedings of the 27th ICRC*, Hamburg, 2001, pp. 4063–4066.

Shea, M.A., Smart, D.F., and McCracken, K.G., A study of vertical cutoff rigidities using sixth degree simulations of the geomagnetic field, *J. Geophys. Res.*, 1965, vol. 70, pp. 4117–4130. doi 10.1029/JZ070i017p04117

Smart, D.F. and Shea, M.A., World grid of calculated cosmic ray vertical cutoff rigidities for epoch 1990.0, *Proceedings of the 25th ICRC*, vol. 2, Durban, 1997, pp. 401–404.

Smart, D.F. and Shea, M.A., World grid of calculated cosmic ray vertical cutoff rigidities for epoch 1995.0, *Proceedings of the 30th ICRC*, vol. 1, Mexico, 2007a, pp. 733–736.

Smart, D.F. and Shea, M.A., World grid of calculated cosmic ray vertical cutoff rigidities for epoch 2000.0, *Proceedings of the 30th ICRC*, vol. 1, Mexico, 2007b, pp. 737–740.

Smart, D.F., Shea, M.A., and Flückiger, E.O., Magnetospheric models and trajectory computations, *Space Sci. Rev.*, 2000, vol. 93, no. 1, pp. 305–333. doi 10.1023/A:1026556831199

Tsyganenko, N.A., A magnetospheric magnetic field model with a warped tail current sheet, *Planet. Space Sci.*, 1989, vol. 37, no. 1, pp. 5–20. doi 10.1016/0032-0633(89)90066-4

Tsyganenko, N.A., A model of the near magnetosphere with a dawn–dusk asymmetry: 1. Mathematical structure, *J. Geophys. Res.*, 2002a, v. 107, no. A8, pp. SMP12-1–SMP12-5. doi 10.1029/2001JA000219

Tsyganenko, N.A., A model of the near magnetosphere with a down–dusk asymmetry: 2. Parameterization and fitting to observations, *J. Geophys. Res.*, 2002b, vol. 107, no. A8, pp. SMP10-1–SMP10-17. doi 10.1029/2001JA000220

Tsyganenko, N.A., Data-based modelling of the Earth's dynamic magnetosphere: A review, *Ann. Geophys*. 2013, vol. 31, pp. 1745–1772. doi 10.5194/angeo-31-1745-2013

Tsyganenko, N.A. and Sitnov, M.I., Modeling the dynamics of the inner magnetosphere during strong geomagnetic storms, *J. Geophys. Res.*, 2005, vol. 110, A03208, pp. 1–16. doi 10.1029/2004JA010798

Tsyganenko, N.A. and Stern, D.P., Modeling the global magnetic field of the large-scale Birkeland current systems, *J. Geophys. Res.*, 1996, vol. 101, pp. 27187–27198. doi 10.1029/98JA02292

Xu, W.-Y., Wei, Z., and Ma, S., Dramatic variations in the Earth's main magnetic field during the 20th century, *Chin. Sci. Bull.*, 2000, vol. 45, no. 21, pp. 2013–2016. doi 10.1007/BF02909699

Zreda, M., COSMOS project, Cutoff rigidity online calculator, model IGRF, University of Arizona, 2012. http://cosmos.hwr.arizona.edu/Util/rigidity.php.

Translated by O. Pismenov